Soft Matter

Cite this: *Soft Matter*, 2012, **8**, 4890

www.rsc.org/softmatter

COMMUNICATION

Cylinder-to-gyroid phase transition in a rod–coil diblock copolymer†

Shih-Hsiang Lin,‡ Chun-Chih Ho‡ and Wei-Fang Su*

Received 27th December 2011, Accepted 20th March 2012
DOI: 10.1039/c2sm07473g

In this communication, the morphology of well-defined P3DDT-*b*-PMMA with a 65.2% PMMA coil volume fraction is revealed as a hexagonally packed cylinder structure by X-ray scattering experiments after thermal annealing. Upon heating, an order-to-order transition (OOT) between cylindrical and gyroidal structures is observed at temperatures above 170 °C. The evolution of the cylinder to the gyroid occurs while the crystalline structure of the P3DDT block disappears, suggesting the conformation of the P3DDT-*b*-PMMA at high temperatures is similar to coil–coil block copolymers. The phenomena reported here can provide a different viewpoint of the self-assembly behaviors of poly(3-alkylthiophene)-containing rod–coil block copolymers. The novel rare gyroid structure of this rod–coil copolymer is useful to fabricate long sought of bicontinuous structure for highly efficient polymer solar cells.

Controlling the ordered and continuous nanoscale morphology of the active layer *via* solvent or thermal annealing is one of the approaches to achieve high performance organic optoelectronics.[1] As block copolymers (BCPs) can self-assemble thermodynamically into a variety of periodic nanostructures on the 10 nm scale[2] and transfer from one phase to another under external conditions,[3,4] they become very promising materials for improving device efficiency.[5,6] Recently, the relationship between morphology and performance of BCPs as the active layer has been investigated for organic optoelectronics.[7,8] The way to enhance the performance of device relies not only on ordered nanostructures of block copolymers but also on their orientations. Among the morphologies of BCPs, the gyroid is one of the most appealing nanostructures for applications in organic optoelectronics due to its unique bicontinuous geometry and interpenetrating networks in the three-dimensional space between electrodes.

Poly(3-alkylthiophene) (P3AT)s are widely investigated and utilized in devices because of their high charge mobility ($\sim 10^{-2}$ cm^2 V^{-1} s^{-1}),[9] and therefore the ordered nanomorphology of P3AT-containing BCPs would be a promising strategy for the fabrication organic optoelectronics. For this purpose, a variety of poly(3-hexylthiophene) (P3HT)-based rod–coil block copolymers have been synthesized recently.[10–15] However, the morphology of P3HT-containing rod–coil or coil–rod–coil block copolymers are usually observed in wire or lamellae.[16–19] This phenomenon might be attributed to the strong rod–rod interaction which would dominate the self-assembly of P3HT-containing rod–coil BCPs.[20]

The self-assembled behaviors of rod–coil BCPs have been investigated in detail based on model DEH–PPV-based block copolymers with different segregation strengths in the past years, and are strongly associated with the Flory–Huggins (rod–coil) interaction (χ), Maier–Saupe (rod–rod) interaction (μ) and the competition between μ and χ ($G = \mu/\chi$).[21–24] If G is large, which means the Maier–Saupe (rod–rod) interaction would dominate, only lamellar phases are observed across the entire volume fraction.[21] Whereas if the G value decreases with increasing Flory–Huggins (rod–coil) interaction, a variety of nanostructures are obtained.[22–24] The nematic phase was absent since conjugated rods were confined within the nanodomain.[24] At a specific coil volume fraction around the phase boundary, even an order-to-order transition (OOT), from a hexagonal to a lamellar nanostructrue, was found in rod–coil BCPs.[22] It is important to understand the effect of chemical structure of the rod block on the self-assembly of rod–coil block copolymers.

The presence of coil segments in rod–coil block copolymers has an influence on the charge mobility in comparison with homo conducting polymers.[25] While there is an interesting strategy to remove the insulating coil segment and then back-fill the acceptor materials into the vacancy of the nanostructure of the etched-BCPs,[26,27] ordered and continuous morphology with high a mobility of the active layer of devices could be obtained. In terms of this point, polylactide (PLA)[26–31] or poly(methyl methacrylate) (PMMA)[32] can be chosen as good candidate of coil segments because they can be easily removed by etching with NaOH or by UV irradiation, respectively. For etched block copolymer films, however, the maintenance of ordered nanostructures is crucial to have a good performance in solar cells.[26,27] The P3AT-based block copolymer with a gyroidal structure could be maintained without collapse after etching one segment because of the fine, interpenetrating and bicontinuous characteristics of the gyroid.

Considering the advantages mentioned above, herein, we introduce a longer side chain, dodecyl, instead of hexyl at the 3-position of the thiophene ring in order to suppress the rod–rod interactions, which resulting in fiber morphologies. A well-defined and low polydispersity rod–coil block copolymer, poly(3-dodecylthiophene)-*b*-poly(methyl methacrylate) (P3DDT-*b*-PMMA), was successfully prepared by using GRIM and anionic polymerization respectively,

Department of Materials Science and Engineering, National Taiwan University, 1, Roosevelt Road, Section 4, Taipei-106, Taiwan. E-mail: suwf@ntu.edu.tw; Fax: +886-2-23634562; Tel: +886-2-33664078

† Electronic supplementary information (ESI) available. See DOI: 10.1039/c2sm07473g

‡ These authors contributed to this work equally.

followed by "click" chemistry. The self-assembly behavior of this copolymer was investigated using small-angle X-ray scattering, wide-angle X-ray scattering (WAXS) and transmission electron microscopy (TEM). Both the cylindrical and gyroid phases were clearly observed for the copolymer containing a 65.2% volume fraction of PMMA.

The synthesis and characterization of P3DDT-*b*-PMMA (as shown in Fig. 1) are described in detail in the supporting information.† The morphology of this copolymer was investigated by using small-angle X-ray scattering (SAXS) and transmission electron microscopy (TEM). The sample was first annealed at 200 °C for one day under an inert atmosphere. Finally, the crystallite of the P3DDT block was reorganized by annealing at 70 °C for another day. For the SAXS measurement at 30 °C, the rod–coil block polymer shows a hexagonal nanostructure in long-range order with peaks at q values of 1, √3, √4, √7 and √12. The peaks are highly distinguishable, as shown in Fig. 2a. The hexagonal nanostructure observed at a 65.2% volume fraction of P3DDT-*b*-PMMA is quite consistent with that of the similar volume fraction of coil–coil block copolymer systems.[4] The primary peak is centered at a q value of 0.244 $nm^{-1,}$ which corresponds to ~25.75 nm domain spacing. The hexagonal structure can be further confirmed using the TEM technique. For the TEM study, a bulk sample was microtomed to less than 100 nm and stained by RuO_4, so we can distinguish PMMA from P3DDT as light PMMA-rich nanodomains and dark P3DDT-rich nanodomains. Fig. 2b indicates that the copolymer exhibits hexagonal close-packed cylinder (HCP) with two grains. In one grain, the long axes of P3DDT cylinders are perpendicular to the plane of the TEM image. The long axes of the P3DDT cylinders are parallel to the plane of the TEM image in the other grain. The morphology observed in the TEM image is consistent with the SAXS result. The domain size calculated from the TEM image is around 25.8 nm which is close to the value calculated from the SAXS profile. Such a structure is also found in our previous study of P3HT-*b*-P2VP rod–coil block copolymers with a 75% P2VP weight fraction.[11]

The crystalline structure of P3DDT chains in the block copolymer was studied by wide-angle X-ray scattering (WAXS) at different temperatures and differential scanning calorimetry (DSC) as shown in Fig. S6† in the supporting information. For the WAXS measurement, (100) reflection is observed at 2.33 nm^{-1}, corresponding to the interlayer arrangement of 2.70 nm lattice spacing in P3DDT-*b*-PMMA at 30 °C. The (200), (300) and (020) reflections of P3DDT-*b*-PMMA are not obvious and are much smaller than that of homo P3DDT, which may result from a less of a chain organization in the confined cylindrical nanostructure of P3DDT-*b*-PMMA as sketched in Fig. S6a.† Upon heating to 70 °C, the intensity of the reflections started to decrease. On further increasing the temperature up to 100 °C, all reflections of the P3DDT block disappeared due to its crystals completely melting and transforming into the isotropic phase. The results indicate the melting point of the P3DDT main chain is in the range of 70 °C to 100 °C. The DSC thermograms of the P3DDT homopolymer and P3DDT-*b*-PMMA block copolymer are shown in Fig. S6b.† The broad peak of homo P3DDT between 40 and 80 °C is attributed to the melting of the crystallized dodecyl side chains, which is consistent with previous work.[20,33] For the block copolymer, glass transition of the PMMA block is observed at around 120 °C, indicating phase separation occurs in the copolymer. However, it is noted that the melting point of the P3DDT block in the copolymer is shifted to a lower temperature around 97 °C, as compared to that of homo P3DDT (~154 °C). The melting transition for the dodecyl side chain of the P3DDT block is not observed. This DSC result is in agreement with above discussed results of WAXS. The melting enthalpy of the P3DDT block in the copolymer (0.79 J g^{-1}) is much smaller than that of the P3DDT homopolymer

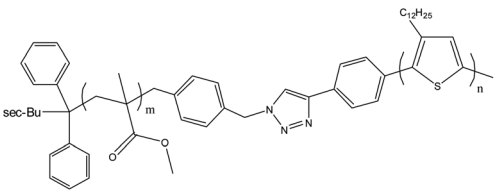

Fig. 1 P3DDT-*b*-PMMA rod–coil block copolymer *via* "click" chemistry.

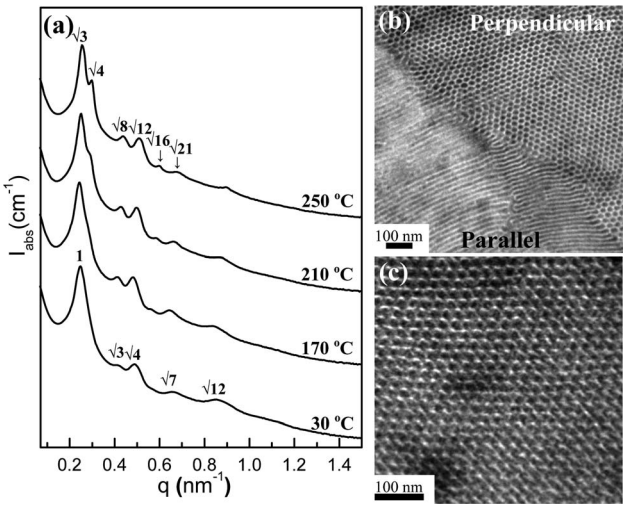

Fig. 2 Morphology studies of a P3DDT-*b*-PMMA block copolymer with a 65.2% volume fraction of PMMA. (a) SAXS profiles at different temperatures, the evolution from cylinder to gyroid occurred between 170 °C and 250 °C. TEM images with RuO_4 staining revealed (b) the sample with cylindrical morphology at 30 °C (dark P3DDT-rich nanodomains and light PMMA-rich nanodomains), and (c) the sample with gyroidal structure quenched from 250 °C.

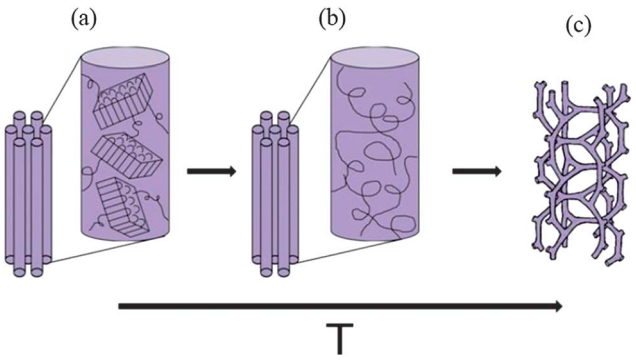

Fig. 3 Schematic illustrations of (a) possible P3DDT segment packing and order-to-order phase transition from (b) cylinder to (c) gyroid in P3DDT-*b*-PMMA rod–coil block copolymer with a 65.2% PMMA coil volume fraction.

(16.57 J g^{-1}), suggesting the poor crystalline structure of P3DDT block is present within the constrained hexagonal nanodomains of P3DDT-*b*-PMMA (Fig. 3a). Moreover, it also indicates no *c*-axis of the P3DDT block is parallel to the cylindrical direction and the *c*-axis may somewhat incline to it. Both WAXS and DSC results show the significant low melting temperature of the P3DDT block and almost no reflection positions changed as opposed to the P3DDT homopolymer. Besides, homo P3DDT exhibits the melting peak with shoulder. According to previous work,[33] the shoulder near the main melting peak is related to the transition of a noninterdigitated P3DDT crystalline structure (Phase I) → nematic mesophase, while the main melting peak corresponds to the isotropic phase of the homo P3DDT. We did not observe the shoulder in our copolymer which may be due to the crystallization of P3DDT constrained within the cylindrical nanodomain. There is limited space within the cylindrical domain to arrange the P3DDT rods in the same direction and form the nematic phase. Further investigation of the crystalline orientations in the nanodomain of this copolymer is ongoing.

As we described before, the P3DDT block completely melted above 100 °C. Therefore, there is a possible phase transformation from a hexagonal structure with crystalline P3DDT in the cylindrical nanodomains to a hexagonal structure with an amorphous P3DDT block upon heating as sketched in Fig. 3 (from Fig. 3a to Fig. 3b). To investigate the phase transition of this block copolymer, we have studied its SAXS profiles under various temperatures as shown in Fig. 2a. When the temperature increased to 170 °C, a small bump adjacent to the primary peak was observed. On further increasing the temperature, this bump finally transformed into a sharp peak at 250 °C, suggesting another phase transition occurred from 170 °C. The SAXS profile shows clear high-order peaks at √3, √4, √8, √12, √16, and √21 indicative that the rod–coil block copolymers are self-assembled into the gyroid phase in the long-range order. The thermal decomposition temperatures of this block copolymer and its corresponding homopolymers are higher than 300 °C, as shown in Fig. S7.† To avoid any decomposition of the polymers, we didn't heat the sample higher than 290 °C to achieve the isotropic block copolymer. The gyroid structure was further confirmed by TEM studies. The TEM sample was prepared from the bulk sample by annealing at 200 °C for one day, further annealing at 250 °C for 30 min and then quenched by iced water to freeze the desired structure. As shown in Fig. 2c, both the (211) and (220) reflections of the gyroid structure are observed, which are consistent with the TEM images of known coil–coil block copolymers.[34] The cylinder-to-gyroid phase transition observed in the rod–coil block copolymer is similar to the SAXS results of the P3HT-*b*-P2VP block copolymer.[35] The sequence of phase transition observed upon heating from hexagonally packed cylinders to gyroid contradicts the SCFT prediction[36] of the coil–coil BCPs, which would suggest the following sequence, gyroid to hexagonally packed cylinders. This might be due to the effect of fluctuations from the inadequacy of theoretical prediction.[3] The detail for the transition mechanism from cylinder to gyroid has been proposed by some research groups through experimental observations.[37,38]

The microphase order-to-order transition temperature (OOT) is characterized by the appearance of new characteristic peaks in the SAXS profiles. To find the divergence of primary peak intensity and domain spacing, the transition temperature can also be quantified through discontinuities in a plot of inverse intensity and domain spacing of primary peak *versus* inverse temperature as shown in Fig. 4. The starting temperature of the divergence of primary peak intensity and domain spacing is found at around 170 °C. The evolution of the transition temperature finishes at around 222 °C. The windows of the hexagonally packed cylinder structure and gyroid structure are separated by the region of the transition temperatures. The phase transition from one microstructure to another could lead to the change in domain spacing, as shown in Fig. 4b. Opposing to the domain spacing of the hexagonal phase, the gyroid phase has a slightly smaller domain spacing, which is shifted from 25.75 to 24.65 nm. The slight change in domain spacing might be associated with a small curvature change from the cylinder to gyroid phase. It is different from the phase transition between hexagonal structure to lamellar structure with a large curvature change, resulting in a large domain spacing change for a rod–coil block copolymer.[22] The small change in domain spacing was also observed in the lamellae-to-gyroid phase transition in aqueous solution[39] and in the cylinder-to-gyroid phase transition[3] for a coil–coil block copolymer. It is worth to note that the crystalline structure of the P3DDT block is already melted while the gyroid structure is forming. Since the gyroid structure possesses high geometric curvature, the conformation of the P3DDT-*b*-PMMA at high temperatures should be similar to that of conventional coil–coil block copolymers.

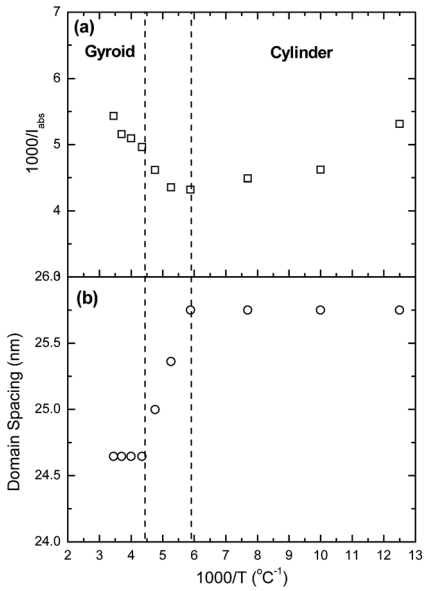

Fig. 4 Determination of order-to-order phase transition of the P3DDT-*b*-PMMA rod–coil diblock copolymer. (a) Inverse SAXS intensity and (b) domain spacing (nm) in the vicinity of the order-to-order transition (OOT). The discontinuity in the slope of the inverse intensity *versus* inverse temperature curve indicates the order-to-order transition. The area between dashed lines indicates the cylinder-to-gyroid phase transition region around from 170 to 222 °C.

Through the data analysis of SAXS, WAXS and DSC results, we can illustrate the phase transition of P3DDT-*b*-PMMA rod–coil block copolymers as shown in Fig. 3. The P3DDT-*b*-PMMA (a 34.8 : 65.2 volume fraction) rod–coil block copolymer is self assembled into a hexagonal structure with the crystalline P3DDT segments confined in the nanocylinder (Fig. 3a). With increasing temperature, the crystalline P3DDT segments melt in the cylindrical domain (Fig. 3b). Upon further heating, the nanostructure

transforms from hexagonal to gyroid morphology (Fig. 3c). The mobility of poly(3-alkylthiophene) is related to its crystallinity and crystal orientation which are key points to determine the performance of optoelectronic devices.[40] Therefore, the results shown here have demonstrated the capability to manipulate the crystalline structure of conjugated polymers within a variety of self-assembled confined nanostructures, which has potential applications in the fabrication of high performance devices.

In conclusion, the well-defined poly(3-dodecylthiophene)-*b*-poly(methyl methacrylate) (P3DDT-*b*-PMMA) rod–coil block copolymer has been successfully synthesized *via* click chemistry, with a 65.2% PMMA volume fraction. The ordered hexagonal close packed cylinder nanostructure was observed at room temperature using both small-angle X-ray scattering (SAXS) and transmission electron microscopy (TEM). The melting point of this copolymer was much lower than that of homo P3DDT, suggesting the crystallites of the P3DDT block could be confined into cylinder nanodomains, which is consistent with the results of wide-angle X-ray scattering (WAXS) at different temperatures. Upon heating the copolymer from 170 to 250 °C, an order-to-order phase transition, from cylinder to gyroid, in the region around from 170 to 222 °C was observed using SAXS. This study provides a different viewpoint of the self-assembly behaviors of poly(3-alkylthiophene)-containing rod–coil block copolymers. The novel, rare bicontinuous gyroid structure of this copolymer is useful to fabricate highly efficient polymer solar cells.

Acknowledgements

We gratefully acknowledge the financial support from the National Science Council of Taiwan (NSC 99-2221-E-002-020-MY3, 99-2120-M-002-011, 100-3113-E-002-012, 100-2120-M-002-007). We also thank Dr U-Ser Jeng, Dr Chun-Jen Su, Dr Jey-Jau Lee and Dr Ming-Tao Lee for helping with SAXS/WAXS experiments at the National Synchrotron Radiation Research Center, Taiwan.

Notes and references

1 J. Peet, M. L. Senatore, A. J. Heeger and G. C. Bazan, *Adv. Mater.*, 2009, **21**, 1521–1527.
2 F. S. Bates, *MRS Bull.*, 2005, **30**, 525–532.
3 G. Floudas, R. Ulrich and U. Weisner, *J. Chem. Phys.*, 1999, **110**, 652–663.
4 K. Schmidt, C. W. Pester, H. G. Schpberth, H. Zettl, K. A. Schindler and A. Boker, *Macromolecules*, 2010, **43**, 4268–4274.
5 R. A. Segalman, B. McCullough, S. Kirmayer and J. J. Urban, *Macromolecules*, 2009, **42**, 9205–9216.
6 I. Botiz and S. D. Darling, *Mater. Today*, 2010, **13**, 42–51.
7 Y. F. Tao, B. McChullough, S. Kim and R. A. Segalman, *Soft Matter*, 2009, **5**, 4219–4230.
8 E. J. W. Crossland, M. Nedelcu, C. Ducati, S. Ludwigs, M. A. Hillmyer, U. Steiner and H. J. Snaith, *Nano Lett.*, 2009, **9**, 2813–2819.
9 I. Osaka and R. D. McCullough, *Acc. Chem. Res.*, 2008, **41**, 1202–1214.
10 M. C. Iovu, M. Jeffries-EL, E. E. Sheina, J. R. Cooper and R. D. McCullough, *Polymer*, 2005, **46**, 8582–8586.
11 C. A. Dai, W. C. Yen, Y. H. Lee, C. C. Ho and W. F. Su, *J. Am. Chem. Soc.*, 2007, **129**, 11036–11038.
12 N. Sary, F. Richard, C. Brochon, N. Leclerc, P. Leveque, J. N. Audinot, S. Berson, T. Heiser, G. Hadziioannou and R. Mezzenga, *Adv. Mater.*, 2010, **22**, 763–768.
13 H. C. Moon, A. Anthonysamy, Y. Lee and J. K. Kim, *Macromolecules*, 2010, **43**, 1747–1752.
14 Z. Li, R. J. Ono, Z. Q. Wu and C. W. Bielawski, *Chem. Commun.*, 2011, **47**, 197–199.
15 Z. Q. Wu, R. J. Ono, Z. Chen, Z. Li and C. W. Bielawski, *Polym. Chem.*, 2011, **2**, 300–302.
16 C. R. Craley, R. Zhang, T. Kowalewski, R. D. McCullough and M. C. Stefan, *Macromol. Rapid Commun.*, 2009, **30**, 11–16.
17 T. Higashihara and M. Ueda, *React. Funct. Polym.*, 2009, **69**, 457–462.
18 H. Lim, K. T. Huang, W. F. Su and C. Y. Chao, *J. Polym. Sci., Part A: Polym. Chem.*, 2010, **48**, 3311–3322.
19 H. C. Moon, A. Anthonysamy, J. K. Kim and A. Hirao, *Macromolecules*, 2011, **44**, 1894–1899.
20 V. Ho, B. W. Boudouris and R. A. Segalman, *Macromolecules*, 2010, **43**, 7895–7899.
21 B. D. Olsen and R. A. Segalman, *Macromolecules*, 2005, **38**, 10127–10137.
22 B. D. Olsen and R. A. Segalman, *Macromolecules*, 2007, **40**, 6922–6929.
23 N. Sary, L. Rubatat, C. Brochon, G. Hadziioannou, J. Ruokolaonen and R. Mezzenga, *Macromolecules*, 2007, **40**, 6990–6997.
24 C. C. Ho, Y. H. Lee, C. A. Dai, R. A. Segalman and W. F. Su, *Macromolecules*, 2009, **42**, 4208–4219.
25 J. Liu, E. Shina, T. Kowalewski and R. D. McCullough, *Angew. Chem., Int. Ed.*, 2002, **41**, 329–332.
26 I. Botiz and S. B. Darling, *Macromolecules*, 2009, **42**, 8211–8217.
27 I. Botiz, A. B. F. Martinson and S. B. Darling, *Langmuir*, 2010, **26**, 8756–8761.
28 B. W. Boudouris, C. D. Frisbie and M. A. Hillmyer, *Macromolecules*, 2008, **41**, 67–75.
29 B. W. Boudouris, C. D. Frisbie and M. A. Hillmyer, *Macromolecules*, 2010, **43**, 3566–3569.
30 G. Grancharov, O. Coulembier, M. Surin, R. Laazaroni and P. Dubois, *Macromolecules*, 2010, **43**, 8957–8964.
31 V. Ho, B. W. Boudouris, B. L. McCulloch, C. G. Shuttle, M. Burkhardt, M. L. Chabinyc and R. A. Segalman, *J. Am. Chem. Soc.*, 2011, **133**, 9270–9273.
32 U. Jeong, D. Y. Ryu, J. K. Kim, D. H. Kim, X. Wu and T. P. Russell, *Macromolecules*, 2003, **36**, 10126–10129.
33 V. Causin, C. Maraga, A. Marigo, L. Valentini and J. M. Kenny, *Macromolecules*, 2005, **38**, 409–415.
34 S. Akasaka, T. Okamoto, T. Osaka, T. Matsushita and H. Hasegawa, *Eur. Polym. J.*, 2011, **47**, 651–661.
35 Y. H. Lee, W. C. Yen, W. F. Su and C. A. Dai, *Soft Matter*, 2011, **7**, 10429–10442.
36 M. W. Matsen and F. S. Bates, *Macromolecules*, 1996, **29**, 1091–1098.
37 H. Takagi, K. Yamamoto, S. Okamoto and S. Sakurai, *Polymer*, 2010, **51**, 4160–4168.
38 C. Y. Wang and T. P. Lodge, *Macromolecules*, 2002, **35**, 6997–7006.
39 I. Hamley, V. Castelletto, O. O. Mykhaylyk and Z. Yang, *Langmuir*, 2004, **20**, 10785–10790.
40 M. Aryal, K. Trivedi and W. H. Hu, *ACS Nano*, 2009, **3**, 3085–3090.